Structural basis for partial agonist action at ionotropic glutamate receptors

Rongsheng Jin[1], Tue G Banke[3], Mark L Mayer[4], Stephen F Traynelis[3] & Eric Gouaux[1,2]

An unresolved problem in understanding neurotransmitter receptor function concerns the mechanism(s) by which full and partial agonists elicit different amplitude responses at equal receptor occupancy. The widely held view of 'partial agonism' posits that resting and active states of the receptor are in equilibrium, and partial agonists simply do not shift the equilibrium toward the active state as efficaciously as full agonists. Here we report findings from crystallographic and electrophysiological studies of the mechanism of activation of an AMPA-subtype glutamate receptor ion channel. In these experiments, we used 5-substituted willardiines, a series of partial agonists that differ by only a single atom. Our results show that the GluR2 ligand-binding core can adopt a range of ligand-dependent conformational states, which in turn control the open probability of discrete subconductance states of the intact ion channel. Our findings thus provide a structure-based model of partial agonism.

Ligand-gated ion channels are multi-subunit, allosteric proteins that undergo agonist-promoted conformational changes between closed and open states[1]. The earliest mechanistic framework for agonist action suggested that binding and receptor activation were different steps, leading to the distinction between 'agonist affinity' and 'agonist efficacy'[2]. Receptors were thought to exist in conformationally and functionally distinct inactive and active states[3], with the binding of agonist promoting an increase in the relative proportion of the active state[4]. These concepts contributed to the formation of the Monod-Wyman-Changeux (MWC) model of allosteric proteins[5], which predicts that partial agonists shift inactive receptors toward the active state less efficiently than do full agonists. In contrast to the MWC model, the Koshland-Nemethy-Filmer (KNF) theory asserts that receptors undergo sequential, non-concerted changes[6], with different ligands inducing specific and perhaps different conformational states. According to extensive kinetic analysis of voltage-activated *Shaker* potassium channels and Ca^{2+}-activated potassium channels, activation proceeds as a series of transitions through discrete states linked by an MWC-like mechanism[7–9]. For ligand-gated ion channels, similar models have been proposed, but there is insufficient experimental evidence to accurately define the gating process.

Ionotropic glutamate receptors (iGluRs) are ligand-gated ion channels that couple the energy of agonist binding at the ligand-binding core to the opening of a transmembrane ion pore[10]. AMPA-subtype iGluRs mediate most of the fast excitatory synaptic transmission in the mammalian brain and have been the focus of extensive pharmacological scrutiny[11]. iGluRs, which likely comprise four subunits, have semi-autonomous membrane-spanning and ligand-binding domains (**Fig. 1a**)[10]. AMPA receptors are

appropriate for studying the molecular basis of partial agonism because the function of individual receptors can be measured by single-channel recording, and the ligand-binding core can be genetically excised and studied by high-resolution crystallographic techniques[12,13].

Previous studies show that kainate behaves as a partial agonist at AMPA receptors[12,14,15], and mutations in the agonist binding site alter the relative efficacy of AMPA, glutamate and kainate[16]. Interpreting these studies is complicated, however, by the fact that AMPA, kainate and glutamate are chemically distinct and bind to different sub-sites within the ligand binding pocket. Furthermore, compared with other agonists, kainate stabilizes a unique conformational state of the ligand-binding core due to the presence of its pyrrolidine ring and isopropenyl group. Although the aforementioned studies help to explain the action of kainate on AMPA receptors, the mechanism by which partial agonists produce submaximal responses remains to be determined. Such an analysis would be facilitated by studies in which subtle and graded conformational changes in the ligand-binding core are correlated with changes in activity at the ion channel. In this regard, we have found that the 5-substituted willardiines (**Fig. 1b**)[17–19], variations on the parent willardiine from *Acacia willardiana* and *Mimosa asperata*[20], are ideal tools for elucidating the molecular basis of partial agonist action at AMPA receptors. Previous studies have shown that willardiines are partial agonists and that they result in graded levels of desensitization as a consequence of single-atom substitutions. Here we present crystallographic and physiological studies on the GluR2 ligand-binding core and on the intact receptor with a series of willardiine compounds. Our data show that the 5-substituted willardiines stabilize distinct conformational sub-states of the lig-
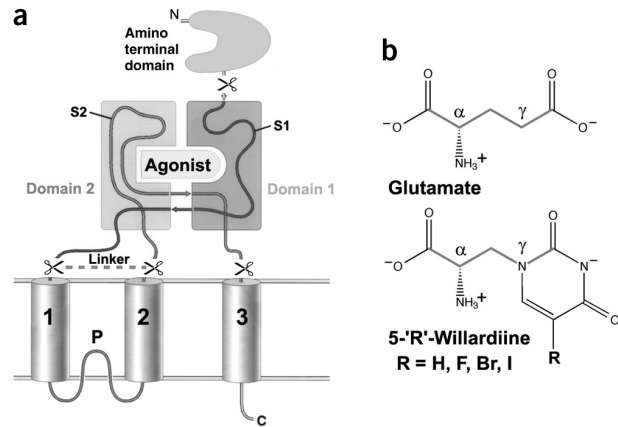
Figure 1 Ionotropic glutamate receptor domain organization and agonist structure. (**a**) iGluR domain organization. Polypeptide segments S1 and S2 comprise the water-soluble, ligand-binding core and the S1S2J construct studied here includes residues 392–506 (S1) and 632–775 (S2) linked together by a Gly–Thr dipeptide. The amino terminal domain (ATD) and the transmembrane segments are not contained within the S1S2J construct. (**b**) Chemical structures of glutamate and 5-substituted willardiines.

and-binding core that are directly related to the level of receptor activation and desensitization.

RESULTS

Single-atom substitutions affect activation and desensitization

In dose-response analyses by two-electrode voltage clamp on *Xenopus laevis* oocytes expressing the L483Y nondesensitizing GluR2 point mutant[21], 5-substituted willardiines yielded EC_{50} values of 6.34, 0.19, 0.84 and 1.51 μM for HW, FW, BrW and IW, respectively (**Fig. 2a**). In parallel experiments on homomeric wild-type GluR2 receptors using saturating concentrations of 5-substituted willardiines and studied under conditions with desensitization intact or blocked by cyclothiazide, we found that the maximal response varied systematically. Increasing the size of the 5-substituent yielded progressively smaller current responses (H > F > Br > I) in the presence of cyclothiazide, and the current amplitudes were 0.62, 0.54, 0.37 and 0.34 for HW, FW, BrW and IW, respectively, normalized to the glutamate response (**Fig. 2c,d**). Similar results were also obtained from the same series of compounds when desensitization was blocked by the L483Y mutation (data not shown). By con-

trast, the amplitudes of the plateau or steady-state currents following the onset of desensitization, in the context of the wild-type receptor, showed the reverse order (I > Br > F > H), with values of 2.23, 1.75, 1.19 and 0.85 for IW, BrW, FW and HW, respectively, normalized to the steady-state current for glutamate (**Fig. 2c,d**). These data, in conjunction with previous experiments on native receptors[18,19], suggest that the capacity of the 5-substituted willardiines to activate and desensitize the GluR2 receptor is correlated with the size of the 5-substituent. In a ligand-displacement assay using [³H]-AMPA and the GluR2 ligand-binding core, IC_{50} values of 4.76 μM, 23.53 nM, 0.30 μM and 0.52 μM for HW, FW, BrW and IW were obtained (**Fig. 2b**). Thus, the rank-order of potency more closely matches the electronegativity of the 5-substituent than its size, suggesting that the electronegativity, which alters the pK_a value of the uracil ring, is the main determinant of potency, as proposed previously[18,19].

Willardiines induce distinct conformations of ligand-binding core

To understand how the 5-substituted willardiines interact with the ligand-binding core of the GluR2 receptor, we determined high-resolution co-crystal structures with each of the four willardiine compounds. Representative electron density maps are shown in **Fig. 3** for all four willardiine complexes. Crystallographic statistics are shown in **Table 1** and **Supplementary Tables 1** and **2** online. All of the co-crystal structures had unambiguous density for the partial agonists and

Figure 2 The 5-substituted willardiines are highly potent agonists and act as partial agonists on the GluR2 receptor. (**a**) Concentration response curves for activation of the non-desensitizing L483Y mutant of the GluR2 receptor by willardiines; data points shown are means ± s.e.m. of responses from two-electrode voltage-clamp experiments performed on five oocytes normalized to the maximum response for individual agonists. (**b**) Competition by willardiines for [³H]-AMPA binding, as measured by filter binding assays. The results are the average of two duplicate experiments. The error bars represent the standard deviation. (**c**) Records from two-electrode voltage-clamp experiments carried out on wild-type GluR2 with saturating concentrations of glutamate and willardiines. Left, experiments were carried out under non-desensitizing conditions in the presence of 100 μM cyclothiazide; right, experiments performed under desensitizing conditions, in the absence of cyclothiazide. (**d**) Graphical summary of data from five oocytes illustrating the reciprocal relationship between peak and steady-state currents.
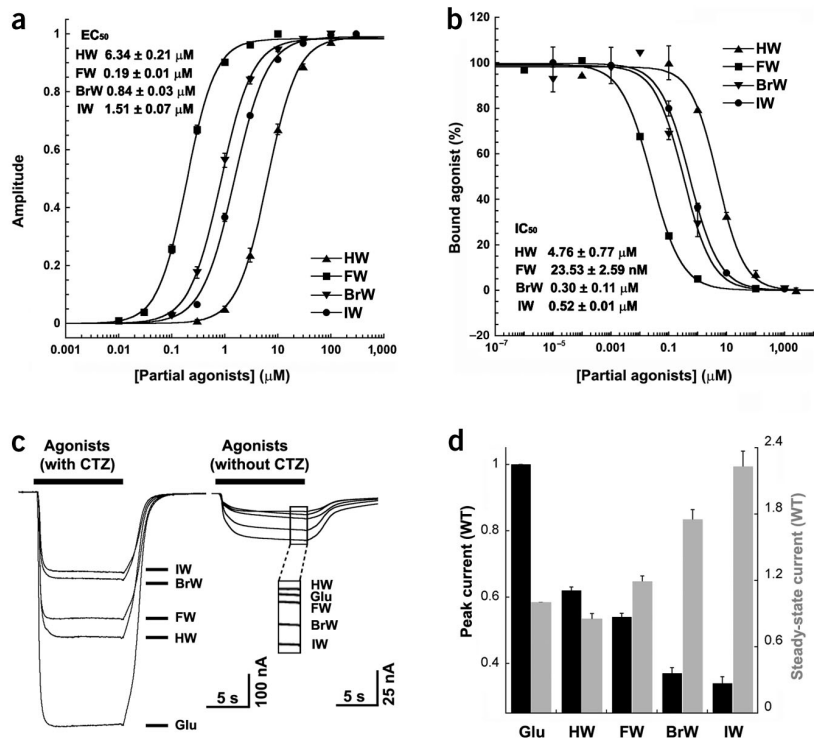
Figure 3 Electron density $|F_o| - |F_c|$ 'omit' maps for willardiines and selected interacting residues. (**a**) HW complex. (**b**) FW complex. (**c**) BrW complex. (**d**) IW complex. Maps are contoured at 4.0σ for HW, FW and BrW complexes, and 3.2σ for IW complex.

binding site residues. The mode by which the willardiines bind to the ligand-binding core is similar to that of glutamate[12]: the α-carbon substituents superimpose within experimental error, and the atoms at the 2 and 3 positions of the willardiine ring occupy the same positions as the atoms in the γ-carboxylate group of glutamate. However, the uracil-like ring and the 5-substituents produce substantial and important structural changes in the ligand-binding pocket. (See **Supplementary Fig. 1** online for the ligand-binding pocket in the superimposed glutamate and willardiines complexes.)

An increase in the size of the 5-substituent results in a striking and graded increase in cleft opening between domains 1 and 2 of the ligand-binding core (**Fig. 4**). Full agonists, such as glutamate, quisqualate and AMPA induce the greatest domain closure. The 5-substituted willardiines, which are partial agonists, stabilize more open domain conformations. Relative to the glutamate-bound complex, in which we observed ~20° of domain closure[12], the HW complex is 3.4° more open and the IW bound form is 9.2° more open. Because the ligand-binding cores in the intact receptor are organized as a pair of 'back-to-back' dimers[13], the degree of domain closure of the agonist binding cleft is coupled to an increase in the intra-dimer separation of the portion of domain 2 that is proximal to the ion channel, at Pro632 (**Fig. 4c,d**). We suggest that the separation of the regions near Pro632 'pulls' the ion channel gate open and that the greater the separation, the greater the extent of ion channel activation (**Fig. 4e**). Because the 5-substituted willardiines produce submaximal domain closure, they in turn result in submaximal separation of the regions near Pro632, and therefore submaximal ion channel activation (**Fig. 4d**).

Single-channel analysis

How do the graded conformational changes induced by binding of different partial agonists lead to activation of distinct-amplitude macroscopic currents? Do receptors populate the same set of subconductance states as full agonists but with different relative frequencies or open times[22,23]? To address this question, we first performed a fluctuation analysis of macroscopic current responses of the non-desensitizing homomeric GluR2-L483Y receptor[21] to the slow application of maximally effective concentrations of glutamate, IW and HW in outside-out membrane patches. Sequential application of different agonists onto the same patch produced a range of response amplitudes similar to those observed in experiments on oocytes. Analysis of the current variance yielded a strong correlation between the maximal response amplitude and the weighted mean
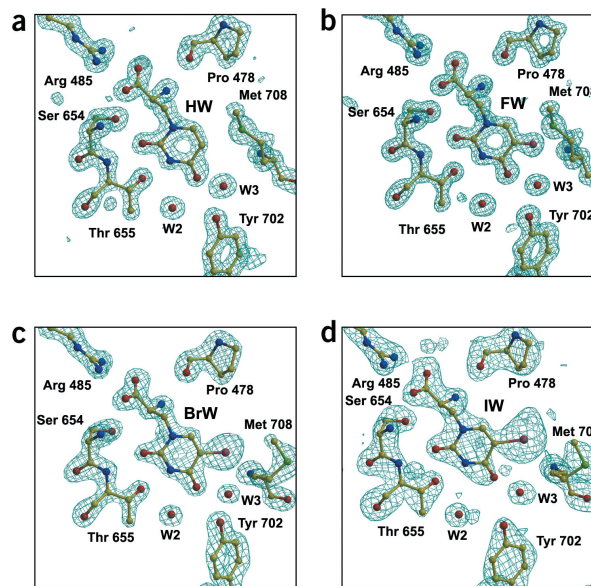
conductance, with glutamate, HW and IW producing current responses with weighted mean conductances of 13.1, 11.6, and 7.2 pS ($n = 10$–12 patches per agonist), respectively (**Supplementary Table 3** and **Supplementary Fig. 3** online). These data suggest that the reduced efficacy of the 5-substituted willardiines relative to glutamate reflects the activation of open states with a different average conductance. To determine the amplitude and duration of the open states activated by glutamate and 5-substituted willardiines, we carried out single-channel analysis of steady-state responses.

Sequential application of a saturating concentration of glutamate or IW to the same outside-out patch containing wild-type GluR2 receptors produced discrete openings to multiple subconductance levels (**Fig. 5a,b**). We analyzed the combined data from five patches that had low enough channel density so that individual openings could be clearly resolved. These measurements reveal that glutamate and IW activate open states with the same conductance values but different relative frequencies (**Tables 2** and **3**). Similar results were obtained from five patches sequentially challenged with glutamate and BrW (**Tables 2** and **3**). Open-duration histograms describing glutamate-, BrW- and IW-evoked unitary currents could be fitted with two exponential components (**Fig. 5c,d** and **Table 2**). The slower time constant primarily describes openings to the lowest subconductance level (6.5 pS, **Fig. 5c,d**). Using time-course fitting to analyze simulated ion channel activity with subconductance levels and noise and filtering added to reproduce experimentally observed responses, we found that the apparent three-fold longer open duration of the 6.5 pS sublevel reflects an inability to resolve both brief openings as well as brief closures that would otherwise subdivide a single apparent opening into two briefer openings. This slower time constant provides a convenient signature for low-amplitude events, and its relative proportion is incrementally increased for BrW and IW (**Table 2**). These data suggest that full and partial agonist binding to GluR2 leads to differential activation of a set of shared open states that exhibit common subconductance levels.

Table 1 Refinement statistics

Ligands	Resolution (Å)	R_{work}[a] (%)	R_{free}[b] (%)	Average B-value		r.m.s. deviations	
				Overall	Ligand	Bonds Å	Angles(°)
HW	30–1.65	20.8	22.9	18.97	13.08	0.006	1.22
FW	30–1.35	19.9	21.8	15.95	8.27	0.005	1.22
BrW	30–1.80	19.8	23.1	20.35	15.53	0.005	1.21
IW	30–2.15	18.8	23.7	24.84	29.80	0.006	1.24

[a]$R_{work} = (\Sigma||F_o| - |F_c||)/\Sigma|F_o|$, where F_o and F_c denote observed and calculated structure factors, respectively.
[b]Ten percent of the reflections were set aside for the calculation of the R_{free} value.
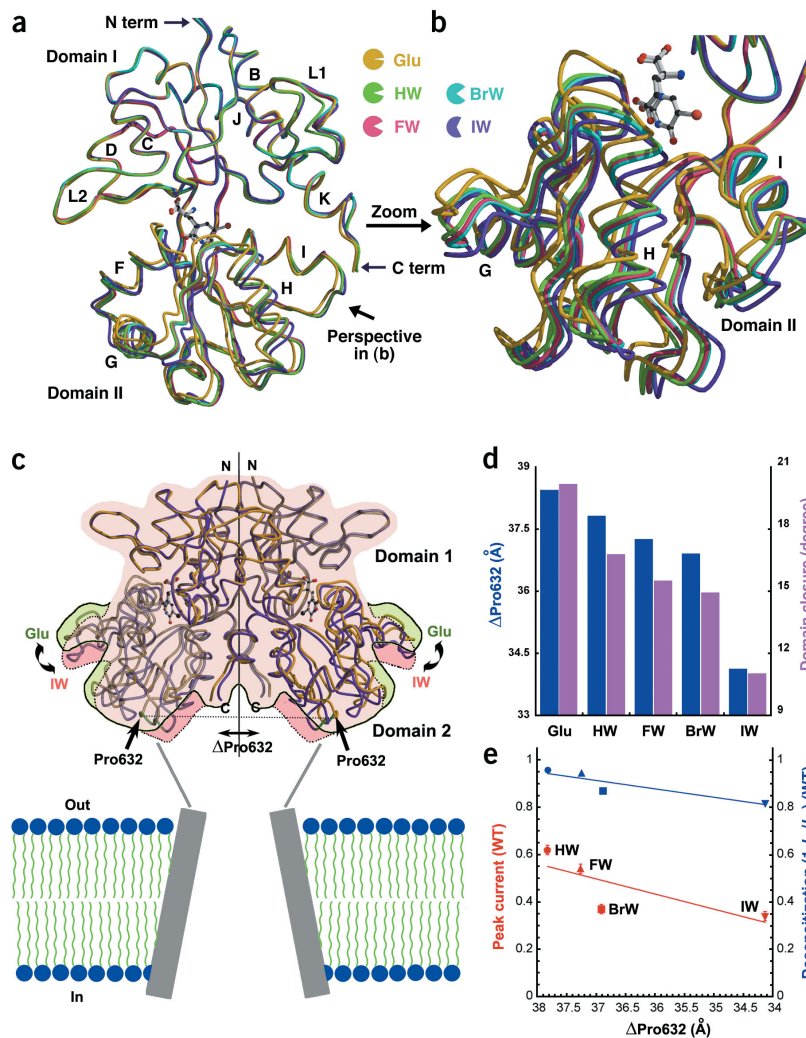
Figure 4 The 5-substituted willardiines produce greater domain closure and separation of residue Pro632 as the size of the 5-substituent decreases. (**a**) Superposition of the structures of the GluR2 ligand-binding core in complexes with glutamate (yellow), HW (green), FW (red), BrW (cyan) and IW (purple) using main-chain atoms in domain 1. Glutamate and IW are shown in ball-and-stick representation. (**b**) Close-up view of domain 2 derived from the superimposed structures in **a**. Note the spectrum of conformational states from the glutamate-bound form to the IW bound state. (**c**) The dimer of the ligand-binding core in the activated, non desensitized state illustrating how the increase in domain closure of individual subunits, with the glutamate and IW complexes as examples, results in a corresponding increase in the separation between the linker regions of each subunit. The outlines of the glutamate and IW dimers are in green and pink, respectively. (**d**) Illustration of how greater domain closure is correlated to greater separation between Pro632 residues in the ligand-binding core dimer. (**e**) Graphical representation of the correlation between the separation of Pro632 in the dimer in the HW, FW, BrW and IW structures and the corresponding maximum current response and extent of desensitization. I_{ss} is the current amplitude for the steady state response on the wild-type receptor and I_{pk} is the peak current for the wild-type receptor in the presence of cyclothiazide.

predicted proportions of subconductance levels using the experimentally determined values of ε for glutamate (0.67), BrW (0.53) and IW (0.40). The similar weighted mean conductances for glutamate responses measured from single-channel currents (12.7 pS), non-stationary variance analysis of wild-type GluR2 currents (14.0 ± 1.2 pS; $n = 7$) and sta-

Definition of coupling efficiency

To relate the change in single-channel properties to the distinct structural states of the ligand-binding core, we developed a model of GluR2 function in which a single parameter describes how individual agonists can cause the differential occupancy of a common set of shared subconductance levels. We assumed that the 6.5, 11.2 and 17.9 pS subconductance levels of GluR2-L483Y receptors (see Methods) arise when 2, 3 or 4 subunit-associated gates are open, respectively[24,25]. We propose that there is no current flow when all gates are closed, and that opening of a single gate either produces no current flow or unitary currents that are too small to resolve. We define the coupling efficiency (ε) as the probability that each independent subunit-associated gate within the receptor complex can open when an agonist molecule is bound (**Fig. 6a**), and we assume all subunits operate independently. Using the binomial expansion, we can estimate the relative proportions of each of five different states of the receptor (0, 1, 2, 3 or 4 gates activated) for coupling efficiencies between 0 and 1, assuming that different conductance levels possess similar open times. We have compared these probabilities and the experimentally determined relative proportions of subconductance levels to determine the best values of ε for glutamate, IW and BrW. **Table 3** shows excellent correspondence between the observed and

tionary variance analysis of GluR2-L483Y currents (13.1 ± 0.8 pS, $n = 11$; **Fig. 6b**) suggests that the same subconductance levels are shared by GluR2 and GluR2-L483Y.

We subsequently used our estimation of ε for glutamate (0.67) to calculate coupling efficiencies for all of the 5-substituted willardiines using their measured relative efficacy at GluR2-L483Y in oocytes or HEK cells. To do this we used the probabilities of the three conductance levels described by this model when $\varepsilon = 0.67$ to estimate the relative amplitude of the glutamate response, and then varied ε between 0 and 1 to generate a full range of predicted partial agonist responses. We plotted the ratio of the predicted partial agonist responses ($\varepsilon = 0$ to 1) to the glutamate response for $\varepsilon = 0.67$ (**Fig. 6b**, smooth line). Comparison of the measured ratios of response amplitudes in oocytes (BrW, FW) and HEK cells (IW, HW) to this predicted response ratio allows us to estimate values of ε for these partial agonists (**Fig. 6b**). There was excellent correspondence between ε calculated independently from IW- and BrW-activated single channels (0.40, 0.53) and macroscopic IW- and BrW-current amplitudes relative to glutamate (0.41, 0.52), further supporting our conclusions. The coupling efficiency (ε) for glutamate and all four 5-substituted willardiines shows excellent correlation with the extent of domain closure determined from the structural data (**Fig. 6c**).

Figure 5 Partial agonists differentially activate subconductance levels. (**a**,**b**) Representative GluR2 single-channel currents were activated by saturating concentrations of IW (150 µM) and glutamate (1 mM) in the same outside-out patch. The amplitude histograms for this patch are shown in the lower panels; baseline noise is superimposed with r.m.s. value. Amplitude distributions were fitted by the maximum likelihood method with the sum of three Gaussian components with the standard deviation constrained to be equal. Sublevel amplitudes were identical for the two agonists. (**c**,**d**) Open period distributions for all sublevels are shown for 150 µM IW and 1 mM glutamate. Data are pooled from five patches that were sequentially exposed to glutamate and IW, and fitted with the sum of two exponential components. Data are shown on a square-root scale; area in gray indicates events briefer than 1 filter rise time (~0.33 ms), which were not fitted. Thin line shows the open period histogram for the lowest subconductance level determined using an Acrit of 1.00 pA; the data were fitted by a single exponential component.
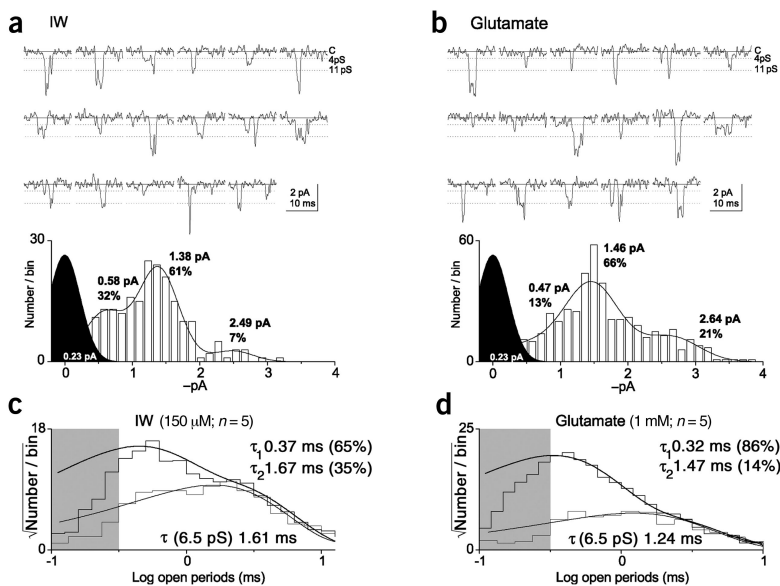
DISCUSSION

A long-standing question in understanding neurotransmitter receptor function concerns the molecular mechanism underlying agonist action. Despite a wealth of functional data on glutamate receptor full and partial agonists, distinguishing between the MWC model (differential equilibrium distribution between shared states) and the KNF model (different agonist-induced conformations) has remained unresolved for decades. The structural comparison between the full agonists glutamate and AMPA, and the partial agonists kainate and Br-HIBO provided the initial clues that agonists with different efficacy induce distinct conformations in a semi-autonomous domain of the receptor, the S1S2 ligand-binding core[12,26]. Unfortunately, because the partial agonists used in these previous studies were substantially different in structure from either glutamate or AMPA, they occupied different sub-sites in the ligand-binding pocket and induced distinct conformations of the ligand-binding core. Therefore, it was difficult to convincingly relate changes in the conformation of the ligand-binding core to alterations in the activity of the ion channel. Furthermore, the functional experiments that accompanied the structural work only dealt with macroscopic currents, leaving the underlying molecular mechanism of ion channel gating unresolved. Indeed, the lack of structural and functional data from a suitable series of partial agonists has been a major obstacle in understanding the basis of partial agonism in glutamate receptors[27]. Here we studied the 5-substituted willardiines and have found that the size of a single

substituent incrementally controls the degree of domain closure in the ligand-binding core and, in turn, the extent of receptor activation and desensitization.

The high-resolution crystal structures reported here show that the willardiines all have similar molecular interactions with the receptor, but each willardiine derivative causes the ligand-binding core to adopt a distinct conformation due to the size of the 5-substituent, consistent with KNF theory. When the size of the 5-substituent increases in the order of H < F < Br < I, the GluR2 ligand-binding core adopts an increasingly more open domain conformation and a shorter intra-dimer separation proximal to the ion channel gate. Indeed, comparison of the structural and functional data obtained from the GluR2 ligand-binding core shows that the degree of domain closure and intra-dimer separation are correlated to the extent of receptor activation and desensitization (**Fig. 4e** and **Supplementary Fig. 2** online). The most parsimonious explanation for this correlation is that the agonist-dependent intra-protein forces that trigger channel opening are also directly related to the molecular rearrangements of the dimer interface that lead to desensitization. Therefore, as activation becomes energetically less favorable, as in the case of IW, desensitization is also proportionally less favorable. In molecular terms, we suggest that agonist binding and the resulting domain closure of the ligand-binding core exerts 'strain' on both the gate of the ion channel and on the dimer interface. Thus, either the ion channel opens or the dimer interface rearranges, resulting in activation or desensitization, respectively.

Table 2 Single-channel properties[a]

	Glutamate	BrW	IW
Sublevel-1 ($\gamma1$)	6.1 pS	5.3 pS	6.5 pS
Sublevel-1 ($\gamma2$)	11.4 pS	10.8 pS	11.2 pS
Sublevel-1 ($\gamma3$)	18.0 pS	17.1 pS	17.8 pS
$Tau1_{OPEN}$, Area	0.3 ms, 83%	0.5 ms, 77%	0.4 ms, 65%
$Tau2_{OPEN}$, Area	1.5 ms, 17%	2.5 ms, 23%	1.7 ms, 35%

[a]Single-channel currents were recorded in outside-out patches in response to maximally effective concentrations of glutamate (1 mM), IW (150 µM) or BrW (80 µM) applied successively to each of five patches. Data for glutamate are the average from fits to two data sets, each from five patches.

Table 3 Comparison of observed and predicted sublevel frequencies

	ε[a]	6.5 pS		11.2 pS		17.9 pS	
		Obs.[b]	Pred.[b]	Obs.	Pred.	Obs.	Pred.
Glutamate	0.67	27%	33%	53%	45%	20%	22%
BrW	0.53	55%	51%	33%	38%	12%	11%
IW	0.40	63%	66%	33%	29%	4%	5%

[a]ε is the coupling efficiency defined as the probability that each independent subunit-associated gate within the receptor complex can open when an agonist molecule is bound.
[b]Obs. and Pred. stand for the observed and predicted sublevel frequencies, respectively.

Figure 6 Subunit-linked channel opening is correlated with degree of domain closure. (**a**) We modeled the function of homomeric GluR2-L483Y receptors by assuming that each of four agonist-bound subunits undergoes a conformational change that influences the permeation properties of the channel. The coupling efficiency ε describes the probability that an independent subunit-dependent change that influences permeation will occur when an agonist is bound. We assigned the shared IW- and glutamate-activated conductance levels to channel conformations with 2, 3 or 4 subunit-dependent gates open; we assumed the conductance for one subunit-dependent gate open was too low to measure. The probabilities that 0, 1, 2, 3 and 4 independent subunit gates were open were determined using the binomial expansion; * indicates the existence of three different conformations for dimeric channels (only one is shown). (**b**) The response amplitude to the maximal concentration of agonist was calculated from the probability of openings to different subconductance levels as a function of ε (Methods). The smooth line shows the ratio of the response amplitude for ε between 0 and 1 to the glutamate response calculated using ε = 0.67. The symbols show the value for ε that corresponds to the ratio of the response to maximal concentrations of partial agonists to the maximal glutamate response from oocyte or HEK cell data (filled and open symbols, respectively). (**c**) Graphical representation of the correlation between coupling efficiency and ligand binding domain closure.
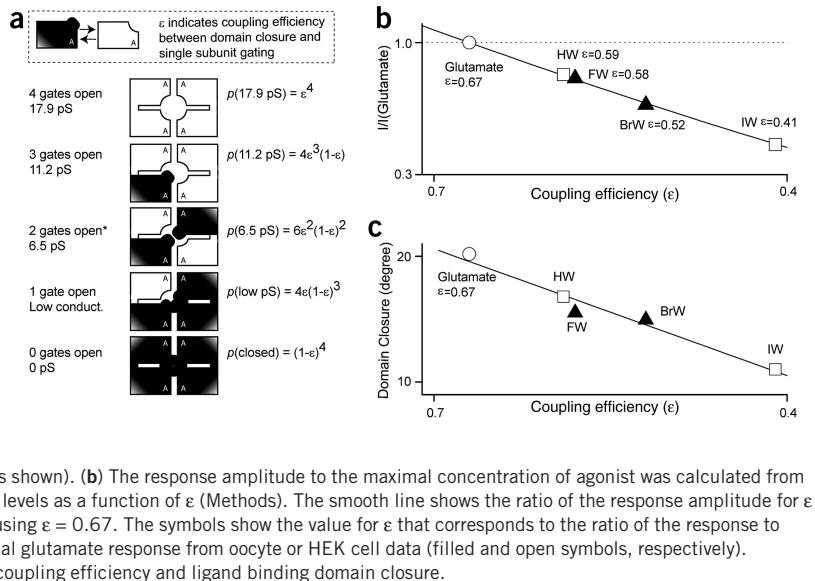
Previous studies emphasize that AMPA receptor activation reflects the opening of subunit-associated gates[23,24]. The homomeric GluR2 receptor used in this study is therefore ideal for comparing structural changes in the ligand binding site to functional changes in the receptor activity. Here we have shown that a single parameter can describe the coupling of agonist binding to one subunit to the opening of its associated gate. Moreover, we have quantified the proportion of activated subunits within a multimeric receptor complex by measuring the conductance level. Our single-channel recordings provide three important insights into the mechanism of partial agonist action. First, partial agonists activate the same open states as glutamate. Second, although partial agonists can populate the highest subconductance state, they preferentially occupy the lower subconductance states, relative to the full agonist glutamate. Third, analysis of the single-channel data allowed us to estimate the coupling efficiency (ε) for several partial agonists. These estimates of coupling efficiency show a striking relation to the degree of domain closure (**Fig. 6c**) and directly suggest that domain closure promotes subunit dependent opening.

Our present results provide the first structure-based model of partial agonism, but there remain caveats to our conclusions. First, we do not yet know the relationship between different degrees of domain closure in crystals and the frequency and extent of domain closure in the free-moving receptor. Second, our single-channel measurements cannot resolve the lowest conductance levels, and our model neglects complicating features of channel function such as direct sublevel transitions and agonist-dependent open times. Issues of resolution and missed events further complicate analysis of the data. Despite these caveats, our studies provide an understanding of how saturating concentrations of partial agonists elicit submaximal responses when desensitization is blocked by cyclothiazide or the L483Y mutation. The ability of partial agonists to induce a differential degree of domain closure within the ligand-binding core determines the contribution of each subunit to gating. The nature of AMPA receptor gating, in which different subunits incrementally contribute to pore opening, converts this graded change in domain closure to quantized unitary current as the opening of higher subconductance levels becomes gradually favored with an increase in coupling efficiency between binding and activation for independent subunits. This conceptual model of partial

agonism, which is consistent with structural data and single-channel data, finally provides a physical explanation for agonist efficacy.

METHODS

Electrophysiology. Two different constructs of GluR2 were used in the present studies. One is the flip version of GluR2, with glutamine at the Q/R editing site[28,29], referred to here as wild-type GluR2. The second construct contains a point mutation (L483Y) within the flip version (Q) that confers a non-desensitizing phenotype[21] and is referred to here as GluR2-L483Y. *Xenopus laevis* oocytes were injected with 0.5–2.0 ng of wild-type GluR2 or GluR2-L483Y RNA 3–5 d before experiments were performed under two-electrode voltage clamp at –60 mV using agarose-cushioned microelectrodes filled with 3 M KCl. Ligands were automatically applied in a buffer composed of 100 mM NaCl, 1 mM KCl, 0.5 mM BaCl$_2$, 1 mM MgCl$_2$ and 5 mM HEPES, with the pH adjusted to 7.6. Ligands were employed at concentrations at least 100-fold above their EC$_{50}$ values (**Fig. 2a**) and cyclothiazide was used at 100 μM. Data were acquired and analyzed as previously described[30].

Human embryonic kidney (HEK) cells were maintained and transiently transfected with 2 μg/ml cDNA encoding wild-type GluR2 or GluR2-L483Y[21], together with 0.6 μg/ml cDNA encoding green fluorescent protein, as previously described[31]. Eight hours after transfection, fresh media supplemented with 10 μM 6-cyano-7-nitroquinoxaline-2,3-dione was added. Current responses to rapid and slow agonist application to outside-out patches were recorded under voltage clamp (V_{hold}, –100 mV) the next day, as previously described[31]. Macroscopic data were analyzed using ChanneLab (Synaptosoft) or software developed by the authors. Stationary variance analysis and non-stationary variance analysis of the current response (10 kHz digitization, 5 kHz filter) of wild-type GluR2 and GluR2-L483Y receptors in outside-out patches to maximally effective concentrations of agonist were performed as previously described[31,32].

Simulated bursting and non-bursting channel openings to 6.5, 11.2, 17.9 pS levels (0.5 ms open time; 50 μs interval; ChanneLab) were filtered at 1 kHz, Gaussian noise with r.m.s. of 0.23 pA was added, and the record was analyzed using time course fitting (SCAN provided by D. Colquhoun, University College London[33]). Experimentally recorded single-channel openings in outside-out patches were low-pass filtered at 1 kHz (–3 dB), digitized at 20 kHz and analyzed using time-course fitting. Only patches with low baseline noise (r.m.s. 0.17–0.31 pA; mean 0.23 pA) were analyzed. Application of agonist increased the frequency of detected transitions 15-fold over agonist-free control records, suggesting that < 7% of our lowest amplitude currents may be false events. Patches were sequentially exposed to either 1 mM glutamate and

150 μM IW (*n* = 5; V_{hold}, −100 mV) or 1 mM glutamate and 80 μM BrW (*n* = 5; V_{hold}, −140 mV). Openings from five patches were pooled for each agonist, and openings longer than 2.0 filter rise times (0.66 ms) were used to construct amplitude histograms; only transitions greater than 0.2 pA were considered direct sublevel transitions. Amplitude histograms for glutamate (1,116 and 1,425 openings), IW (1,225 openings), and BrW (1,287 openings) were fitted to the sum of three Gaussian components with the standard deviations constrained to be equal[33]. Because there was no significant difference between wild-type GluR2 sublevel amplitudes activated by glutamate, IW or BrW (**Table 2**), we assumed that these two agonists activate the same sublevels. We therefore fitted the composite histogram of data to three Gaussian components to get the best estimate of the shared subconductance levels. Chord conductance values were calculated at −120 mV for glutamate/IW or −160 mV for glutamate/BrW (measured V_{rev} was +10 mV, corrected for +10 mV junction potential). To obtain an estimate of relative contribution of different sublevels (**Table 3**), we refit histograms for glutamate, IW or BrW with three Gaussian components with the amplitudes constrained to be equal (G1u, IW) or within 5–10% (BrW) of the shared conductance levels (6.5, 11.2 and 17.9 pS); standard deviation was allowed to vary, and ranged between 0.262 and 0.504.

The weighted mean conductance was calculated for values of coupling efficiency ε between 0 and 1 using our measured subconductance levels and the following equation[34]:

$$\gamma_{noise} = \Sigma N p_j \gamma_j^2 / \Sigma N p_j \gamma_j$$

where *N* is the number of channels, γ is conductance, and *p* is the open probability for 6.5, 11.2 and 17.9 pS sublevels determined from the binomial expansion. Coupling efficiency ε for glutamate, BrW and IW were determined by comparing this theoretical relationship to the γ_{noise} determined from single-channel measurements, variance analysis of glutamate activation of non-desensitizing GluR2-L483Y receptors and non-stationary variance analysis of rapid glutamate application to wild-type GluR2 receptors. The response amplitude to maximal concentration of agonist was predicted from the probability of openings to different subconductance levels as a function of ε using

$$\text{Response amplitude} = V \Sigma N p_j \gamma_j$$

where *V* is the driving force, *N* the number of channels, γ the subconductance level and *p* the open probability for 6.5, 11.2 and 17.9 pS sublevels determined from binomial expansion. Values of ε for 5-substituted willardiines were determined independently from the single-channel records or alternatively by comparison of the experimentally determined willardiine/glutamate response ratio and the predicted relationship between ε and response ratio.

A 200-μs resolution was applied to the data and openings to all subconductance levels (0.3–4.0 pA) were used to construct open-duration histograms for glutamate (3,434 and 3,457 openings), IW (2,333) and BrW (1,168). Histograms were fitted by the sum of two exponential components using maximum likelihood methods; only open times longer than one filter rise time (0.33 ms) were fitted. Critical amplitudes were calculated[33] to distinguish open times for different subconductance levels.

Crystallography. The GluR2 S1S2J ligand-binding core construct was expressed, purified and crystallized in the presence of 5 mM HW, 5 mM FW, 10 mM BrW and 10 mM IW. Crystals were grown at 4 °C by hanging drop vapor diffusion containing a 1:1 ratio of protein and reservoir solution. Reservoir solutions were as follows: HW, 14–18% PEG5K MME, 0.1 M zinc acetate and 0.1 M sodium citrate, pH 5.5; FW and BrW, 14–16% PEG8K, 0.2 M sodium chloride and 0.1 M sodium citrate, pH 5.5; IW, 18–22% PEG1K, 0.2 M lithium sulfate and 0.1 M phosphate-citrate buffer, pH 4.2. Prior to flash cooling in liquid nitrogen, the co-crystals were briefly soaked in the corresponding crystallization buffer supplemented with ligand and 12–16% glycerol. The HW and FW data sets were collected at the National Synchrotron Light Source, and the BrW and IW data sets were measured using CuK_{α} radiation at Columbia University. The data sets were processed with the HKL suite of programs[35] and the relevant statistics are provided in **Supplementary Table 1** online.

The FW structure was solved by molecular replacement (MR) with AmoRe[36] using the AMPA complex structure as a search model[12]. The structures of the HW, BrW and IW complexes were determined by MR using the

FW structure as search probe. Refinements were performed with CNS[37], and after rigid body minimization, a slow-cool, simulated-annealing protocol (5000 K; torsion angle dynamics) was performed to minimize model bias. Subsequent rounds of positional refinement and individual temperature factor refinement were combined with manual rebuilding and addition of solvent and ligands until the R_{free} value converged. O software[38] was used for model building, superpositions were calculated with LSQMAN[39], and the extent of domain closure was determined using the program FIT (http://bioinfol. mbfys.lu.se/~guoguang/fit.html). The degree of domain closure was defined as the rotation required to fit domain 2 (Ile500–Lys506, Pro632–Asp728 and the Gly–Thr linker) following superposition of domain 1 (Val395–Phe495 and Tyr732–Tyr768), using α-carbon atoms in the superposition. Because extensive structural studies have shown that full agonists induce similar and full domain closure conformation[12,26,30], and that the apo state is conformationally heterogeneous, here we have defined the extent of domain closure in the willardiine complexes relative to protomer C of the glutamate structure[12]. However, to maintain a common convention with the previous studies, where the degree of domain closure induced by glutamate was shown to be 20.2° relative to the apo complex[12], we define the degree of domain closure for the willardiines as the difference in domain closure between the glutamate-bound protomer C and the willardiine protomer, subtracted from 20.2°. For the IW complex, the degrees of domain closure for the two molecules in the asymmetric unit differ by 0.47°, and the average value was used for further structure and function analyses. We also noticed that in the IW structure, the ligand in molecule B showed multiple conformations (data not shown); and the conformation around the linker region (Lys505–Lys506, Pro632–Glu634) in the molecule B was distorted in comparison to the conformation in molecule A and the other known full and partial agonist structures. We suggest that the dissimilar conformation observed in IW molecule B could be an artifact due to the crystal lattice packing. Therefore, an IW-bound ligand-binding core dimer was generated using two copies of IW molecule A. The separation between residues Pro632 in a ligand-binding core dimer was directly measured as the distance between the corresponding C_{α} atoms. Figures were prepared using MOLSCRIPT[40], BOBSCRIPT[41] and Raster3D[42].

Ligand binding assay. The IC_{50} values were measured for the GluR2 S1S2J construct as previously described[43]. Briefly, for competition binding studies the protein sample was incubated with 20 nM [³H]-AMPA (10.6 Ci/mmol) for one hour on ice in binding buffer (30 mM Tris-hydrochloride, pH 7.2, 100 mM potassium thiocyanate, 2.5 mM calcium chloride and 10% glycerol), together with various concentrations of willardiines (from 1 pM to 2.5 μM). GSWP 02500 membranes were used for filter binding. Ligand binding experiments were carried out in duplicate, and the average of two experiments was reported.

The atomic coordinates for the HW, FW, BrW and IW cocrystal structures have been deposited at the Protein Data Bank under accession codes 1MQJ, 1MQI, 1MQH and 1MQG, respectively.

Note: Supplementary information is available on the Nature Neuroscience website.

1. Hille, B. *Ion Channels of Excitable Membranes* (Sinauer, Sunderland, Massachusetts, 2001).
2. Stephenson, R.P. A modification of receptor theory. *Brit. J. Pharmacol.* **11**, 379–393 (1956).

ARTICLES

3. Wyman, J. & Allen, D.W. The problem of the heme interactions in hemoglobin and the basis of the Bohr effect. *J. Polymer Sci.* **VII**, 499–518 (1951).
4. Del Castillo, J. & Katz, B. Interaction at end-plate receptors between different choline derivatives. *Proc. R. Soc. Lond. B. Biol. Sci.* **146**, 369–381 (1957).
5. Monod, J., Wyman, J. & Changeux, J.P. On the nature of allosteric transitions: a plausible model. *J. Mol. Biol.* **12**, 88–118 (1965).
6. Koshland, D.E., Nemethy, G. & Filmer, D. Comparison of experimental binding data and theoretical models in proteins containing subunits. *Biochemistry* **5**, 365–385 (1966).
7. Schoppa, N.E. & Sigworth, F.J. Activation of shaker potassium channels. I. Characterization of voltage-dependent transitions. *J. Gen. Physiol.* **111**, 271–294 (1998).
8. Cox, D.H., Cui, J. & Aldrich, R.W. Allosteric gating of a large conductance Ca-activated K⁺ channel. *J. Gen. Physiol.* **110**, 257–281 (1997).
9. Horrigan, F.T., Cui, J. & Aldrich, R.W. Allosteric voltage gating of potassium channels I. Mslo ionic currents in the absence of Ca²⁺. *J. Gen. Physiol.* **114**, 277–304 (1999).
10. Dingledine, R., Borges, K., Bowie, D. & Traynelis, S.F. The glutamate receptor ion channels. *Pharmacol. Rev.* **51**, 7–61 (1999).
11. Bräuner-Osborne, H., Egebjerg, J., Nielsen, E. O., Madsen, U. & Krogsgaard-Larsen, P. Ligands for glutamate receptors: design and therapeutic propects. *J. Med. Chem.* **43**, 2609–2645 (2000).
12. Armstrong, N. & Gouaux, E. Mechanisms for activation and antagonism of an AMPA-sensitive glutamate receptor: crystal structures of the GluR2 ligand binding core. *Neuron* **28**, 165–181 (2000).
13. Sun, Y. *et al.* Mechanism of glutamate receptor desensitization. *Nature* **417**, 245–253 (2002).
14. Zorumski, C.F. & Yang, J. AMPA, kainate and quisqualate activate a common receptor-channel complex on embryonic chick motoneurons. *J. Neurosci.* **8**, 4277–4286 (1988).
15. Patneau, D.K. & Mayer, M.L. Kinetic analysis of interactions between kainate and AMPA: evidence for activation of a single receptor in mouse hippocampal neurons. *Neuron* **6**, 785–798 (1991).
16. Armstrong, N., Mayer, M.L. & Gouaux, E. Tuning activation of the AMPA-sensitive GluR2 ion channel by genetic adjustment of agonist-induced conformational changes. *Proc. Natl. Acad. Sci. USA* **100**, 5736–5741 (2003).
17. Evans, R.H., Jones, A.W. & Watkins, J.C. Willardiine: a potent quisqualate-like excitant. *J. Physiol. (Lond.)* **308**, 71P–72P (1980).
18. Patneau, D.K., Mayer, M.L., Jane, D.E. & Watkins, J.C. Activation and desensitization of AMPA/kainate receptors by novel derivatives of Willardiine. *J. Neurosci.* **12**, 595–606 (1992).
19. Wong, L.A., Mayer, M.L., Jane, D.E. & Watkins, J.C. Willardiines differentiate agonist binding sites for kainate-versus AMPA-preferring glutamate receptors in DRG and hippocampal neurons. *J. Neurosci.* **14**, 3881–3897 (1994).
20. Gmelin, R. Isolierung von willardiin (3-(1-uracyl)-L-alanin) aus den samen von *Acacia millefolia*, *Acacia lemmoni* und *Mimosa asperata*. *Acta Chem. Scand.* **15**, 1188–1189 (1961).
21. Stern-Bach, Y., Russo, S., Neuman, M. & Rosenmund, C. A point mutation in the glutamate binding site blocks desensitization of AMPA receptors. *Neuron* **21**, 907–918 (1998).
22. Swanson, G.T., Kamboj, S.K. & Cull-Candy, S.G. Single-channel properties of recombinant AMPA receptors depend on RNA editing, splice variation and subunit composition. *J. Neurosci.* **17**, 58–69 (1997).
23. Smith, T.C., Wang, L.-Y. & Howe, J.R. Heterogeneous conductance levels of native AMPA receptors. *J. Neurosci.* **20**, 2073–2085 (2000).
24. Rosenmund, C., Stern-Bach, Y. & Stevens, C.F. The tetrameric structure of a glutamate receptor channel. *Science* **280**, 1596–1599 (1998).
25. Robert, A., Irizarry, S.N., Hughes, T.E. & Howe, J.R. Subunit interactions and AMPA receptor desensitization. *J. Neurosci.* **21**, 5574–5586 (2001).
26. Hogner, A. *et al.* Structural basis for AMPA receptor activation and ligand selectivity: crystal structures of five agonist complexes with the GluR2 ligand-binding core. *J. Mol. Biol.* **322**, 93–109 (2002).
27. Kizelsztein, P., Eisenstein, M., Strutz, N., Hollmann, M. & Teichberg, V.I. Mutant cycle analysis of the active and desensitized states of an AMPA receptor induced by willardiines. *Biochem.* **39**, 12819–12827 (2000).
28. Boulter, J. *et al.* Molecular cloning and functional expression of glutamate receptor subunit genes. *Science* **249**, 1033–1037 (1990).
29. Keinänen, K. *et al.* A family of AMPA-selective glutamate receptors. *Science* **249**, 556–560 (1990).
30. Jin, R., Horning, M., Mayer, M.L. & Gouaux, E. Mechanism of activation and selectivity in a ligand-gated ion channel: structural and functional studies of GluR2 and quisqualate. *Biochem.* **41**, 15635–15643 (2002).
31. Banke, T.G. *et al.* Control of GluR1 AMPA receptor function by cAMP-dependent protein kinase. *J. Neurosci.* **20**, 89–102 (2000).
32. Traynelis, S.F. & Jaramillo, F. Getting the most out of noise in the central nervous system. *Trends Neurosci.* **21**, 137–145 (1998).
33. Colquhoun, D. & Sigworth, F.J. Fitting and statistical analysis of single-channel records in *Single-Channel Recording* (eds. Sakmann, B. & Neher, E.) 483–587 (Plenum, New York, 1995).
34. Cull-Candy, S.G., Howe, J.R. & Ogden, D.C. Noise and single channels activated by excitatory amino acids in rat cerebellar granule neurones. *J. Physiol.* **400**, 189–222 (1988).
35. Otwinowsky, Z. & Minor, W. Processing of X-ray diffraction data collected in oscillation mode. *Meth. Enzymol.* **276**, 307–326 (1997).
36. Navaza, J. *AMoRe*: An automated package for molecular replacement. *Acta Crystallogr.* **A50**, 157–163 (1994).
37. Brunger, A.T. *et al.* Crystallography & NMR system: a new software suite for macromolecular structure determination. *Acta Crystallogr.* **D54**, 905–921 (1998).
38. Jones, T.A. & Kjeldgaard, M. Electron-density map interpretation. *Meth. Enzymol.* **277**, 173–208 (1997).
39. Kleywegt, G.J. & Jones, T.A. Model building and refinement practice. *Meth. Enzymol.* **277**, 208–230 (1997).
40. Kraulis, P.J. *MOLSCRIPT*: a program to produce both detailed and schematic plots of protein structures. *J. Appl. Cryst.* **24**, 946–950 (1991).
41. Esnouf, R.M. Further additions to MolScript version 1.4, including reading and contouring of electron-density maps. *Acta Crystallogr.* **D55**, 938–940 (1999).
42. Merritt, E.A. & Murphy, M.E.P. *Raster3D* Version 2.0: a program for photorealistic molecular graphics. *Acta Crystallogr.* **D50**, 869–873 (1994).
43. Chen, G.Q. & Gouaux, E. Overexpression of a glutamate receptor (GluR2) ligand binding domain in *Escherichia coli*: application of a novel protein folding screen. *Proc. Natl. Acad. Sci. USA* **94**, 13431–13436 (1997).